

# 32806

by UMB IJIMEAM

---

**Submission date:** 14-Apr-2025 01:38PM (UTC+0700)

**Submission ID:** 2645471828

**File name:** 32806-Pudjiwati-Edited.docx (3.88M)

**Word count:** 5536

**Character count:** 31418

## Use of *Hibiscus rosa-sinensis* as a Green Corrosion Inhibitor for Valve Materials in RO Water

Sri Pudjiwati <sup>1,\*</sup>, Yasa Sanusi <sup>1</sup> and I Gusti Ayu Arwati <sup>1</sup>

<sup>1</sup>Department of Mechanical Engineering, Universitas Mercu Buana, Meruya Selatan, Jakarta 11650, Indonesia  
\*Corresponding Author: pudjiwati@gmail.com (SP)

### Abstract

Valves are mechanical devices that regulate the flow of oil and gas fluids and are typically constructed from materials that are heat-resistant, corrosion-resistant, and capable of withstanding high pressure. However, observations from valve manufacturing companies in the Banten area have shown that valve components made from medium carbon steel ASTM A105N are susceptible to corrosion during hydrotesting, particularly when using reverse osmosis (RO) water as the testing medium. This corrosion can degrade product quality before delivery to customers. To address this issue, this study investigates the use of *Hibiscus rosa-sinensis* as a green corrosion inhibitor. The objective of this research is to evaluate the corrosion rate, inhibitor efficiency, and surface morphology of ASTM A105N valve materials using *Hibiscus rosa-sinensis* in RO water media, with varying inhibitor concentrations and immersion durations. The electrochemical methods used include Potentiodynamic Polarization, Electrochemical Impedance Spectroscopy (EIS), Chronoamperometry, and Scanning Electron Microscopy (SEM). Results from the corrosion rate tests indicated that the highest inhibitor efficiency—59.04%—was achieved at 24 hours of immersion with a 2 g inhibitor concentration. This condition also yielded the lowest corrosion rate of  $1.2231 \times 10^{-2}$  mm/year and the lowest corrosion current ( $i_{cor}$ ) of  $3.2601 \times 10^{-6}$  A/cm<sup>2</sup>. Chronoamperometry testing confirmed these findings with the lowest electric charge value of 0.0125 C. SEM analysis further revealed a more uniform and homogeneous protective coating on the metal surface under these conditions. Based on these results, *Hibiscus rosa-sinensis* demonstrates promising performance as a green corrosion inhibitor and is recommended as an additive in RO water for valve hydrotesting. This study highlights the potential of environmentally friendly and cost-effective inhibitors in reducing corrosion risk in valve materials.

### Article Info:

Received: 14 March 2025  
Revised: 25 March 2025  
Accepted: 8 April 2025  
Available online: 14 April 2025

### Keywords:

Valve material; corrosion rate; ASTM A105N; green inhibitor; *Hibiscus rosa-sinensis*

© 2025 The Author(s).  
Published by Universitas Mercu Buana (Indonesia).  
This is an open-access article under CC BY-SA License.



### 1. Introduction

A valve is a mechanical device that controls the flow of oil and gas fluids by opening, closing, or regulating the flow in a piping system [1], [2]. It plays a vital role in the oil and gas industry [3]. One component of the valve is the closure valve or flange, which connects two parts—between the valve and other components—securely and safely at the end of the pipe [4], [5]. With the flange, the ball valve can be easily accessed for maintenance, replacement, and the assembly or disassembly of system components. Closure valves are designed using heat-resistant, rust-resistant, and high-pressure-resistant materials [6], which provide a strong and leak-proof seal when combined with gaskets and bolts.

However, these combinations—especially those involving gaskets or bolts—may create gaps that can trap air, potentially leading to corrosion. Based on observations in manufacturing companies in the Banten area, the closure valve component is prone to corrosion during leak testing using hydro tests. Residual water trapped in the gaps of the closure valve after testing often causes corrosion [7], which leads to a decrease in quality during delivery.

Corrosion is the deterioration of material quality due to chemical interactions with the surrounding environment [8]. When metal is exposed to humid air, the presence of oxygen can result in corrosion [9]. Additionally, corrosion can disrupt industrial operations and cause financial losses [10], [11]. In other words, corrosion reduces material quality and leads to economic damage [12]. Other studies explain that corrosion on flanges can be caused by CO<sub>2</sub> exposure, high temperatures, high flow rates, and galvanic corrosion, all of which accelerate the corrosion process [13], [14]. Elevated temperatures, in particular, accelerate chemical reactions, leading to faster corrosion rates [15], which can result in material damage and quality degradation [16].

To address these problems, it is essential to identify the causes of corrosion and implement preventive solutions. This includes calculating and selecting corrosion limits on valves by evaluating various process parameters such as scaling, pH regulation, glycol use, and corrosion inhibitors [17]. Corrosion inhibitors are chemical substances added to corrosive environments to slow down or prevent corrosion reactions in metals. These inhibitors form a protective layer on metal surfaces or inhibit the electrochemical processes that cause corrosion [18], [19]. According to the literature, corrosion inhibitors are generally divided into two types: organic and inorganic inhibitors [20], [21]. Organic inhibitors contain phenolic compounds such as tannins, flavonoids, and saponins [22], [23], while inorganic inhibitors do not contain carbon elements in their composition [24], [25]. The use of inhibitors derived from natural materials is considered more advantageous, as they are not only easier to obtain but also more economical and environmentally friendly [26]–[28].

One example of a green inhibitor is *Hibiscus rosa-sinensis*. This plant offers several benefits, including its availability in tropical regions like Indonesia and its low cost. The flowers of *Hibiscus rosa-sinensis* are commonly used in medicinal and cosmetic applications [29], [30]. However, research by Khan et al. (2019) and Stashenco (2023) has shown that *Hibiscus rosa-sinensis* contains flavonoids and tannins, which possess antioxidant and inhibitory properties. These compounds can inhibit oxidation reactions by binding to metal ions and reducing the rate of corrosion. Amines can also form protective layers on metal surfaces. In addition to its use in medicine and cosmetics, several studies have utilized the inhibitory properties of *Hibiscus rosa-sinensis* to prevent corrosion in carbon steel materials, especially low-carbon steel. The results demonstrate that this inhibitor has good efficiency in resisting corrosion on carbon steel [31]–[33], including pipes made from low-carbon steel.

In a study by Nandi et al. (2020), green inhibitors from *Hibiscus rosa-sinensis* leaves achieved an average inhibition efficiency of 89% on mild steel (low-carbon steel) after 24 hours of immersion in hydrochloric acid, sulfuric acid, and phosphoric acid media. Amabou et al. (2024) reported the highest corrosion inhibition efficiency of 93.72% on mild steel using disodium hydrogen phosphate media after 14 days of immersion. Additionally, research by Latha et al. (2024) concluded that *Hibiscus rosa-sinensis* achieved a corrosion inhibition efficiency of 82% on mild steel in an oil well water medium. Based on these findings, along with field observations and interviews with engineering departments at valve manufacturing companies in the Banten area, further research is needed to explore the use of green inhibitors to prevent potential corrosion in valve materials. The researchers believe that the aforementioned green inhibitors have strong potential for application in testing ASTM A105N oil and gas valve materials, particularly for mitigating corrosion in reverse osmosis (RO) water environments.

The purpose of this research is to analyze the corrosion rate, surface morphology, and chemical composition of ASTM A105N valve materials, and to address corrosion problems using green inhibitors—in this case, *Hibiscus rosa-sinensis*. The study investigates the use of inhibitor concentrations of 2 g and 6 g with immersion times of 24 hours, 120 hours, and 240 hours. It is hoped that the results will demonstrate the internal benefits of using green inhibitors for corrosion protection and provide practical recommendations for companies to reduce the risk of corrosion during hydrotesting.

## 2. Methods

This research consists of several stages, starting with a literature study, field data collection, sampling of materials from valve manufacturing companies in the Banten area,

### How to cite:

S. Pudjiwati, Y. Sanusi, and I. G. A. Arwati, "Use of *Hibiscus rosa-sinensis* as a green corrosion inhibitor for valve materials in RO Water," *Int. J. Innov. Mech. Eng. Adv. Mater.*, vol. 7, no. 2, pp. 86-95, 2025

and preparation of tools and materials. The literature study is conducted by gathering data and information from various sources.

Figure 1 illustrates the research method, which begins with a literature review as the foundation for studying and understanding existing research. This is followed by field data collection, which includes gathering information on observed phenomena and obtaining samples for testing. The next stage involves experimental procedures, starting with the preparation of testing tools and materials. Before testing, the samples are cleaned using a NaOH and NaCl solution, followed by degreasing with distilled water. After the testing phase, an evaluation is conducted to analyze the corrosion rate, inhibitor efficiency, and the surface morphology of the test material.

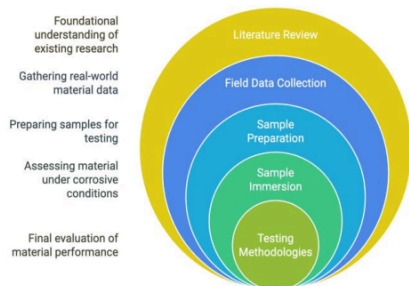


**Figure 1.** Research methodology

### 2.1. Preparation materials

The material used in this research is ASTM A105N, which is commonly used as a base material for valves due to its superior mechanical properties, particularly under high pressure and medium to low temperatures [34].

### 2.2. Sample fabrication process

Figure 2 shows the sample used in this research, which is derived from ASTM A105N valve material. Samples were prepared by cutting the material using a cutting machine into rectangular shapes with dimensions of 20 mm × 10 mm × 2.5 mm [35]. A total of 24 specimens were prepared, with three specimens allocated for each immersion variation. Grit blasting was performed to clean and smooth the metal surface. This process used abrasive paper with grit sizes of 240, 400, and 1000. Grit blasting was conducted in a consistent, unidirectional manner.



Figure 2. Research sample

### 2.3. Sample immersion process

The immersion process was conducted in a mixture of reverse osmosis (RO) water and the green inhibitor *Hibiscus rosa-sinensis*, with inhibitor concentrations of 2 grams and 6 grams, and immersion durations of 24, 120, and 240 hours [35]. Prior to immersion, the samples were degreased using a NaOH solution, treated with NaCl, and rinsed with distilled water (Aquadest) [36]. The pH of the *Hibiscus rosa-sinensis* solution in the RO water was monitored using litmus paper for each inhibitor concentration per Liter of RO water.

### 2.4. Sample testing methodology

#### A. Electrochemical testing methods

The electrochemical testing methods used in this study include potentiodynamic polarization, electrochemical impedance spectroscopy (EIS), cyclic voltammetry, and chronoamperometry. ASTM A105N metal specimens without coatings were electrochemically tested to evaluate their passivation behaviour and corrosion rate. The testing setup is shown in Figure 3. In the electrochemical process, current flows from a positively charged electrode (platinum) to the negatively charged working electrode (ASTM A105N metal).

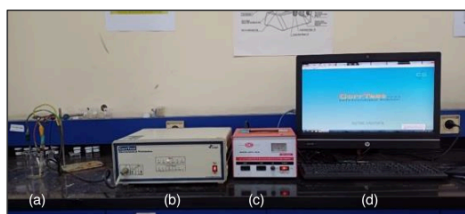


Figure 3. Potentiodynamic polarization testing equipment configuration; (a) Reaction tube with 3 electrodes, (b) Corrtest testing equipment, (c) Voltage stabilizer, and (d) Data recorder

#### B. Potentiodynamic polarization testing

This test used a Corrtest CS 350 potentiostat, as shown in Figure 3. The components include:

- Reaction tube/tank containing three electrodes—working electrode (sample), counter electrode (platinum), and reference electrode (Ag/AgCl)
- Corrtest equipment for data acquisition
- Voltage stabilizer

## (d) PC for real-time data display

The test was conducted using a potential range from -1 V to +1 V with a scan rate of 5 mV/s. The surface area was set at 1 cm<sup>2</sup>, with a metal density of 7.86 g/cm<sup>3</sup>, and the reference electrode correction was set for Ag/AgCl. The working electrode was polished beforehand using 1000-grit abrasive paper. The test results provide data and graphs of potential (V) versus current density (A/cm<sup>2</sup>). Tafel analysis was used to determine the corrosion potential ( $E_{corr}$ ) and corrosion current density ( $i_{corr}$ ), which are used to calculate the corrosion rate.

## C. Electrochemical Impedance Spectroscopy (EIS) testing

EIS was conducted to evaluate the resistance of the metal in the presence of an inhibitor layer. The testing parameters included a frequency range of 0.1 Hz to 1 MHz and an AC amplitude of 10 mV with 6 steps per decade, according to ASTM Standard G106 (1999).

## D. Chronoamperometry testing

Chronoamperometry was used to measure the current response over time at a constant potential. This technique records current and potential data over time and can be used to determine total electric charge. The scan parameters ranged from -0.8 V to +0.2 V versus the reference electrode, with a total testing duration of 60 seconds.

## E. Microscopic testing method using Scanning Electron Microscope (SEM)

Following the electrochemical tests, SEM analysis was conducted to observe the surface morphology of ASTM A105N under various immersion conditions: untreated, immersed for 24 hours in RO water, and immersed for 24 hours in the presence of inhibitors. This analysis provides surface images of the specimens to assess morphological changes after exposure to corrosive environments and electrochemical testing.

### 3. Results and Discussion

#### 3.1. Corrosion rate test result

Table 1 presents the corrosion rate test results, while Figure 4 illustrates the potentiodynamic polarization test results. Figure 4(a) shows the potentiodynamic polarization curve after 24 hours of immersion. The TafelFit analysis yields the following current density ( $i_0$ ) values: without inhibitor =  $3.8141 \times 10^{-6}$  A/cm<sup>2</sup>, with 2 g of inhibitor =  $3.2601 \times 10^{-6}$  A/cm<sup>2</sup>, and with 6 g of inhibitor =  $4.5090 \times 10^{-6}$  A/cm<sup>2</sup>. The corresponding corrosion potential ( $E_0$ ) values are: without inhibitor = -0.31614 V, with 2 g of inhibitor = -0.50501 V, and with 6 g of inhibitor = -0.50263 V. The resulting corrosion rates are: without inhibitor = 0.014310 mm/year, with 2 g of inhibitor = 0.012231 mm/year, and with 6 g of inhibitor = 0.016917 mm/year. Figure 4(b) shows the potentiodynamic polarization results after 120 hours of immersion. The  $i_0$  values are: without inhibitor =  $4.3109 \times 10^{-6}$  A/cm<sup>2</sup>, with 2 g of inhibitor =  $3.8608 \times 10^{-6}$  A/cm<sup>2</sup>, and with 6 g of inhibitor =  $4.0687 \times 10^{-6}$  A/cm<sup>2</sup>. The  $E_0$  values are: without inhibitor = -0.35649 V, with 2 g of inhibitor = -0.46898 V, and with 6 g of inhibitor = -0.45327 V. The corrosion rates are: without inhibitor = 0.016174 mm/year, with 2 g of inhibitor = 0.014485 mm/year, and with 6 g of inhibitor = 0.015265 mm/year. Figure 4(c) presents the corrosion rate and potentiodynamic polarization results after 240 hours of immersion. The  $i_0$  values are: without inhibitor =  $4.4009 \times 10^{-6}$  A/cm<sup>2</sup>, with 2 g of inhibitor =  $3.8582 \times 10^{-6}$  A/cm<sup>2</sup>, and with 6 g of inhibitor =  $4.1325 \times 10^{-6}$  A/cm<sup>2</sup>. The  $E_0$  values are: without inhibitor = -0.21089 V, with 2 g of inhibitor = -0.47682 V, and with 6 g of inhibitor = -0.34177 V. The corrosion rates are: without inhibitor = 0.016551 mm/year, with 2 g of inhibitor = 0.014475 mm/year, and with 6 g of inhibitor = 0.015504 mm/year.

Table 1. Corrosion rate test results

Immersion time Variations (hour)	Variation of Inhibitor Concentration (g/L)	$i_{corr}$ (A/cm <sup>2</sup> )	$E_{corr}$ (V)	Corrosion Rate (mmpy)	Inhibitor Efficiency (IE) (%)
-	No Treatment	$7.9596 \times 10^{-6}$	-0.31023	$2.9939 \times 10^{-2}$	-
24	0	$3.8141 \times 10^{-6}$	-0.31614	$1.4310 \times 10^{-2}$	-

Immersion time Variations (hour)	Variation of Inhibitor Concentration (g/L)	$I_{corr}$ (A/cm <sup>2</sup> )	$E_{corr}$ (V)	Corrosion Rate (mmpy)	Inhibitor Efficiency (IE) (%)
120	2	$3.2601 \times 10^{-6}$	-0.50501	$1.2231 \times 10^{-2}$	59,04
	6	$4.5090 \times 10^{-6}$	-0.50263	$1.6917 \times 10^{-2}$	43,35
	0	$4.3109 \times 10^{-6}$	-0.35649	$1.6174 \times 10^{-2}$	-
	2	$3.8608 \times 10^{-6}$	-0.46898	$1.4485 \times 10^{-2}$	51,50
	6	$4.0687 \times 10^{-6}$	-0.45327	$1.5265 \times 10^{-2}$	48,88
	0	$4.4009 \times 10^{-6}$	-0.21089	$1.6511 \times 10^{-2}$	-
240	2	$3.8582 \times 10^{-6}$	-0.47682	$1.4475 \times 10^{-2}$	51,53
	6	$4.1325 \times 10^{-6}$	-0.34177	$1.5504 \times 10^{-2}$	48,08

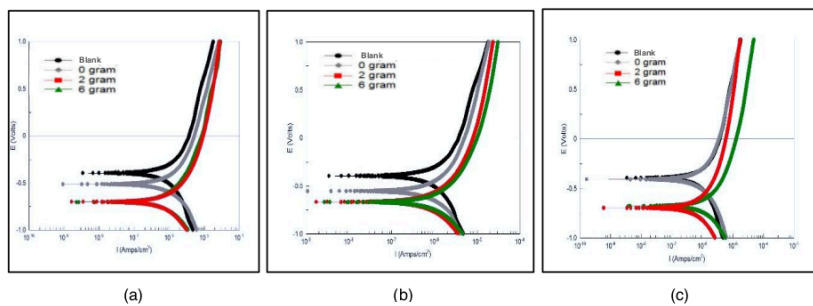


Figure 4. Potentiodynamic polarization graph; (a) Sample with 24 hours immersion, (b) Sample with 120 hours immersion, (c) Sample with 240 hours immersion

The Tafel diagram in Figure 4 shows the results of the potentiodynamic polarization test. This diagram illustrates the relationship between electrochemical potential (E) and the logarithm of current density (log I) in an electrochemical reaction system. From the Tafel diagram, changes in potential and current can be observed after the addition of inhibitors by analyzing the  $E_{corr}$  (corrosion potential) and  $I_{corr}$  (corrosion current density) parameters. The intersection point between the anodic curve (oxidation reaction) and the cathodic curve (reduction reaction) is referred to as the corrosion potential ( $E_{corr}$ ), which represents the natural electrochemical potential of the material in solution without external current. Based on the results of the potentiodynamic polarization test, a decrease in the corrosion current ( $I_{corr}$ ) value was observed after the addition of inhibitors. Specifically, at 24 hours of immersion with a 2-gram inhibitor concentration, the  $I_{corr}$  decreased from  $7.9596 \times 10^{-6}$  A/cm<sup>2</sup> to  $3.2601 \times 10^{-6}$  A/cm<sup>2</sup>, indicating the inhibitor's effectiveness in reducing the corrosion rate. Additionally, the shift in  $E_{corr}$  after inhibitor addition was in the negative direction, from -0.31023 V to -0.50501 V, suggesting that the inhibitor acts as a cathodic type. Based on the Tafel diagram, it can be concluded that *Hibiscus rosa-sinensis* functions as a cathodic inhibitor, as it reduces the electrochemical potential (E) in each sample.

Considering all inhibitor concentrations, there was a decrease in corrosion rate compared to the sample without an inhibitor. The increase in inhibitor concentration led to a reduction in both current and potential, which contributes to the formation of a passive layer and a shift toward a more positive potential—both of which reduce the corrosion susceptibility of the material. This indicates that increasing the inhibitor concentration is effective in reducing corrosion, and the shift in corrosion potential to more negative values suggest a decrease in the likelihood of corrosion. Regarding immersion time, data from the 24-hour immersion tests show that shorter exposure times are more effective in reducing both the corrosion rate and corrosion potential. This suggests that the inhibitor performs better over shorter durations compared to longer immersion times of 120 and 240 hours. However, at a concentration of 6 grams, an increase in corrosion rate was observed, as indicated by a rise in current and potential value shifting closer to the positive direction compared to the 2-gram concentration. This may be due to a drop in the environmental pH from 6 to 5, which increases acidity and negatively impacts the inhibitor's corrosion protection performance.

### 3.2. Inhibitor efficiency

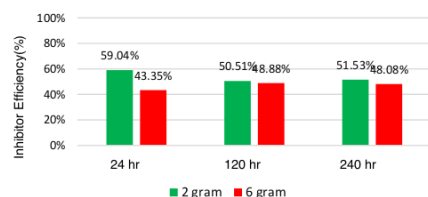


Figure 5. Inhibitor efficiency

Table 1 and Figure 5 compare the results of the inhibitor efficiency (IE) test for samples with inhibitor concentrations of 2 g and 6 g at immersion durations of 24 hours, 120 hours, and 240 hours. From the figure, it is evident that the sample with a 2 g inhibitor concentration at 24 hours of immersion shows the highest inhibitor efficiency, reaching 59.04%.

The inhibitor efficiency is calculated using the following equation [33], [37], [38]:

$$\eta_p = \frac{i_{corr}^0 - i_{corr}}{i_{corr}^0} \times 100\% \quad (1)$$

Where  $\eta_p$  is the inhibitor efficiency in %,  $i_{corr}^0$  is the corrosion current density of the untreated sample ( $7.9596 \times 10^{-6}$  A/cm<sup>2</sup>), and  $i_{corr}$  is the corrosion current density of the sample with the inhibitor layer.

Figure 5 shows the inhibitor efficiency (IE) across various concentrations and immersion times. It can be observed that inhibitor efficiency is influenced by both concentration and immersion duration. The 2 g/L concentration demonstrates better performance than the 6 g/L concentration, achieving an IE of 59.04% at 24 hours of immersion. However, the efficiency at this concentration decreases to 50.51% at 120 hours, then slightly increases to 51.53% at 240 hours—possibly due to inhibitor decomposition or desorption from the metal surface. In contrast, the 6 g/L concentration exhibits a fluctuating pattern: the efficiency increases from 43.35% at 24 hours to 48.88% at 120 hours but then decreases again to 48.08% at 240 hours. This suggests that the interaction between the inhibitor and the solution is less stable at higher concentrations.

Overall, the 2 g/L concentration provides a more stable and moderate efficiency (between 51.05% and 59.04%) throughout the immersion period. Therefore, a 2 g/L concentration is recommended for optimal corrosion protection in short- to medium-duration applications. However, for long-term protection, a more stable inhibitor formulation may be necessary, as the performance of the 6 g/L concentration was less consistent.

### 3.3. Electrochemical Impedance Spectroscopy (EIS) test result

EIS testing measures the system's impedance as a function of the frequency of the applied AC signal. The data obtained is typically analyzed using a Nyquist diagram or Bode diagram to determine parameters such as polarization resistance. In this study, EIS was used to assess the effectiveness of corrosion inhibitors by observing changes in resistance values during testing.

Figure 6 and Table 2 present the results of the EIS tests in the form of Nyquist plots for three conditions: without inhibitors, and with inhibitor concentrations of 2 g and 6 g.

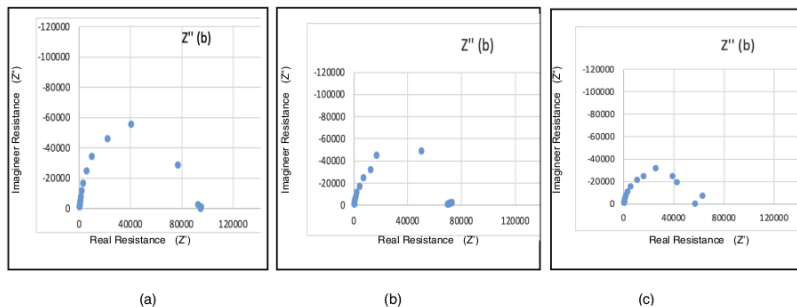


**Figure 6.** Electrochemical Impedance Spectroscopy (EIS) testing; With 24 hours immersion (a), Without inhibitor, (b) Inhibitor concentration 2 gr, and (c) Inhibitor concentration 6 gr

**Table 2.** Electrochemical Impedance Spectroscopy (EIS) test results

Immersion Time Variations (Hours)	Variation of Inhibitor Concentration (g/L)	Largest Real Resistance ( $Z'$ ) ( $\Omega$ )	Largest Imaginary Resistance ( $Z''$ ) ( $\Omega$ )
24	0	94.639	- 55.558
	2	71.422	- 49.288
	6	56.785	- 31.381

Figure 6(a) shows the EIS test results for the sample without an inhibitor. The data points are widely distributed, with the real resistance ( $Z'$ ) reaching approximately 94.639  $\Omega$  and the imaginary resistance ( $Z''$ ) around -55.558  $\Omega$ . This negative resistance is attributed not to the formation of an inhibitor layer, but rather to the presence of a corrosion layer on the metal surface. This is further evidenced by the point distribution in the real resistance area and the low charge transfer resistance ( $R_{ct}$ ), which indicates that an uninhibited and active corrosion process is occurring. Therefore, it can be concluded that no significant inhibitor layer formed in this sample, even though the capacitive behavior of the metal surface still dominates.

Figure 6(b) shows the EIS results for the sample with a 2 g inhibitor concentration. The data points are more concentrated, with a real resistance ( $Z'$ ) around 71.422  $\Omega$  and a higher curvature on the  $Z''$  axis at approximately -49.288  $\Omega$ . This indicates a higher charge transfer resistance compared to the uninhibited sample. Although the data points do not form a complete semicircle, there is a noticeable initial rise followed by spreading, suggesting increased impedance. Higher real resistance implies enhanced resistance to corrosion due to the presence of the inhibitor. Thus, the 2 g inhibitor concentration effectively stabilizes the corrosion inhibition process by slowing down the transfer of ions from the

electrolyte to the metal surface. The larger Nyquist curve indicates better inhibitor performance in forming a protective layer on the metal.

Figure 6(c) shows the EIS results for the sample with a 6 g inhibitor concentration. The real resistance ( $Z'$ ) is lower at around  $56.785 \Omega$  compared to both the 2 g and uninhibited samples. The plot shows only a slight curve at the beginning, indicating a minor increase in charge transfer resistance. The imaginary resistance ( $Z''$ ) is also smaller, around  $-31.381 \Omega$ . This suggests a weaker protective inhibitor layer, likely affected by the immersion medium or environmental conditions. Therefore, the 6 g inhibitor concentration appears to be less effective than the 2 g concentration in forming a stable protective layer. The sample with a 2 g inhibitor concentration is more effective in inhibiting corrosion than the 6 g sample. It shows a higher and more concentrated distribution of data points around the real resistance value, along with a larger Nyquist curve diameter. This implies greater charge transfer resistance and diffusion effects from the inhibitor. The increased resistance in the 2 g sample contributes to a reduced corrosion rate and improved inhibitor performance in forming a protective film on the metal surface.

#### 3.4. Chronoamperometry test result

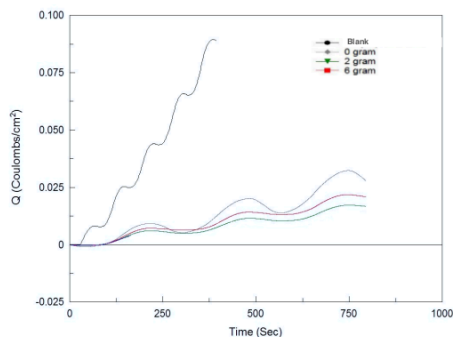


Figure 7. Chronoamperometry test result

Figure 7 presents the results of the chronoamperometry test on samples immersed for 24 hours. The Y-axis represents electric charge ( $Q$ ). The results indicate that the synthetic *Hibiscus rosa-sinensis* inhibitor layer can coat the metal surface and inhibit the flow of electric current, thereby suppressing electrochemical reactions. The lowest electric charge value is observed in the 2 g sample after 24 hours of immersion, suggesting that the inhibitor layer effectively protects the sample surface.

#### 3.5. Scanning Electron Microscope (SEM) test result

SEM analysis was conducted to observe and analyze the surface morphology of the samples. Figure 8 shows SEM images magnified 500x, particularly for the sample with a 2 g inhibitor concentration after 24 hours of immersion.

Figure 8(a) shows the SEM image of a sample without inhibitor treatment, where many fine scratches are visible due to surface polishing with sandpaper. Figure 8(b) displays the surface of a sample immersed in reverse osmosis water without an inhibitor. The surface appears rough and inhomogeneous. Figure 8(c) shows the SEM image of a sample immersed in *Hibiscus rosa-sinensis* solution. The surface appears more homogeneous and is visibly coated with a thin protective film.

These SEM results confirm that the 2 g inhibitor sample forms a smooth, protective layer on the metal surface after 24 hours of immersion. *Hibiscus rosa-sinensis* contains chemical components such as cyanidin, quercetin, hentriacontane, calcium oxalate, thiamine, riboflavin, niacin, and ascorbic acid. These elements are absorbed onto the metal surface during immersion, forming a protective barrier that helps control corrosion.

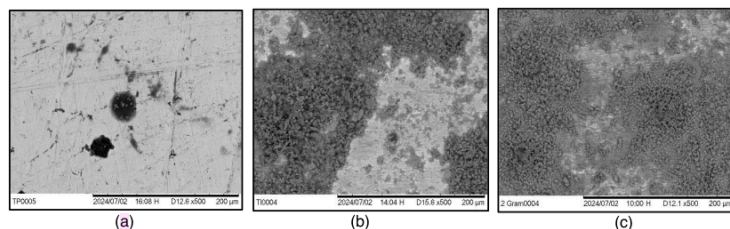


**Figure 8.** SEM test result; (a) Without inhibitor, (b) 2 g inhibitor concentration, and (c) 6 g inhibitor concentration

#### 4. Conclusions

The *Hibiscus rosa-sinensis* flower, as an environmentally friendly green inhibitor, was analyzed through electrochemical and chemical testing to evaluate its effectiveness as a corrosion inhibitor for medium carbon steel ASTM A105N valve material in reverse osmosis (RO) water media. The performance of this green inhibitor showed the highest efficiency at 24 hours of immersion with a 2 g inhibitor concentration, achieving an efficiency of 59.04%, the lowest corrosion rate of  $1.2231 \times 10^{-2}$  mm/year, and the lowest corrosion current ( $i_{corr}$ ) of  $3.2601 \times 10^{-4}$  A/cm<sup>2</sup> compared to other samples. Results from potentiodynamic polarization, electrochemical impedance spectroscopy (EIS), and chronoamperometry tests also indicated that the sample immersed for 24 hours with 2 g of inhibitor had the lowest electrical charge value of 0.0125 C. SEM analysis showed a more uniform and homogeneous coating on the surface of the material. Based on these findings, it can be concluded that *Hibiscus rosa-sinensis* is effective in reducing the corrosion rate of ASTM A105N valve material. Therefore, it is recommended as an additive in RO water during valve hydrotesting. This research highlights the potential benefits of using green inhibitors to reduce corrosion in valve materials. However, to enhance and maintain the inhibitor's long-term efficiency, pH control of the immersion medium is essential. The use of *Hibiscus rosa-sinensis* flower as a green inhibitor effectively reduces the corrosion rate of ASTM A105N valve material and is recommended for use in RO water during hydrotests. This study demonstrates the advantages of environmentally friendly, cost-effective green inhibitors compared to conventional chemical inhibitors in minimizing corrosion potential.

#### References

- [1] G. Gokilakrishnan, S. Divya, R. Rajesh, and V. Selvakumar, "Operating torque in ball valves: A review," *Int J Technol Res Eng*, vol. 2, no. 4, pp. 311–315, 2019.
- [2] K. Sotoodeh, "Failure Mode and Effect Analysis (FMEA) of pipeline ball valves in the offshore industry," *Journal of Failure Analysis and Prevention*, 2020, doi: 10.1007/s11668-020-00924-8.
- [3] K. Sotoodeh, "A review and analysis of industrial valve material failures due to corrosion and proposals for prevention measures based on industrial experiences in the offshore sector of the oil and gas industry," *Journal of Failure Analysis and Prevention*, 2020, doi: 10.1007/s11668-020-01064-9.
- [4] D. W. G. and R. H. Perry, *Perry's Chemical Engineers' Handbook*, 8th Ed., no. 112. New York: McGraw-Hill, 2008.
- [5] H. Wang, L. Zhou, and D. Liu, "Experimental investigation of column separation using rapid closure of an upstream valve," *Applied Sciences (Switzerland)*, vol. 13, no. 23, Dec. 2023, doi: 10.3390/app132312874.
- [6] K. Sotoodeh, "A review of valve stem sealing to prevent leakage from the valve and its effect on valve operation," *Journal of Failure Analysis and Prevention*, 2020, doi: 10.1007/s11668-020-01050-1.
- [7] N. Ji, C. Li, P. Wang, L. Zhu, and C. Feng, "Corrosion cause analysis of a surface pipeline flange corrosion cause analysis of a surface pipeline flange," 2023, doi: 10.1088/1742-6596/2468/1/012171.
- [8] I. Gusti, A. Arwati, S. Alva, A. Fadilah, and Y. Maryani, "Corrosion analysis on aluminum metal (ams 4050) extreme acid rain environment method with weight loss," *World Chemical Engineering Journal*, vol. 5, no. 2, pp. 33–36, 2021, doi: 10.48181/wcej.v5i2.12613.
- [9] I. G. A. Arwati and F. Ifani, "Corrosion rate analysis of JIS G-3141 steel for automotive inner wheel house production with weight loss method," *World Chemical Engineering Journal*, vol. 6, no. 1, p. 1, 2022, doi: 10.48181/wcej.v6i1.14377.
- [10] M. Fontana, *Corrosion Engineering*, McGraw-Hill Book Co., 1987.
- [11] A. Arninda, M. Arnold, S. Ugra, and A. Adawiyah, "Analisa laju korosi dan lifetime material pipa stainless steel 316l di PT Pertamina Geothermal Energy Area Lahendong Sumur LHD 23 Unit 3&4 Cluster 5," *e-Prosiding Seminar Nasional Teknologi Industri VIII*, pp. 389–393, 2021.
- [12] P. Eng. Pierre R. Roberge, Ph.D., *Corrosion Engineering - Practices Vs Principles*. New York: McGraw-Hill Book Co, 2008.

- [13] N. Ji, C. Li, P. Wang, L. Zhu, and C. Feng, "Corrosion cause analysis of a surface pipeline flange," *J Phys Conf Ser*, vol. 2468, no. 1, 2023, doi: 10.1088/1742-6596/2468/1/012171.
- [14] S. Hakimian, A. H. Bouzid, and L. A. Hof, "Effect of gap size on flange face corrosion," *Materials and Corrosion*, no. March, pp. 1–18, 2024, doi: 10.1002/mac0.202414367.
- [15] E. D. Kusumawati and V. P. Fahrani, "Studi baja karbon rendah terhadap laju korosi," *Sprocket Journal of Mechanical Engineering*, vol. 5, no. 2, pp. 59–65, 2024, doi: 10.36655/sprocket.v5i2.1265.
- [16] S. Rossi, F. Russo, A. M. Lemmi, M. Benedetti, and V. Fontanari, "Fatigue corrosion behavior of friction welded dissimilar joints in different testing conditions," *Metals (Basel)*, vol. 10, no. 8, pp. 1–14, 2020, doi: 10.3390/met10081018.
- [17] K. Sotoodeh, "Requirement and calculation of corrosion allowance for piping and valves in the oil and gas industry," *J Bio Tribocorros*, vol. 6, no. 1, pp. 1–8, 2020, doi: 10.1007/s40735-019-0319-4.
- [18] I. G. A. Arwati et al., "Effect of Chitosan on the Corrosion Inhibition for Aluminium Alloy in H<sub>2</sub>SO<sub>4</sub> Medium," *Proceedings of WHEC 2022 - 23rd World Hydrogen Energy Conference: Bridging Continents by H<sub>2</sub>*, pp. 720–722, 2022, doi: 10.3390/en15228511.
- [19] S. Hidayatullah, F. Gapsari, and P. H. Setyarini, "Pengaruh Variasi Konsentrasi Inhibitor dari Kitosan Sisik Ikan terhadap Perilaku Korosi Besi ASTM A36: Study Ekstrapolarisasi Tafel and EIS," *Jurnal Rekayasa Mesin*, vol. 11, no. 1, pp. 51–59, 2020, doi: 10.21776/ub.jrm.2020.011.01.6.
- [20] A. Kadhim, R. Alazawi, and R. H. Abass, "Corrosion inhibitors. A review," *Int. J. Corros. Scale Inhib.*, vol. 10, no. 1, pp. 54–67, 2021, doi: 10.17675/2305-6894-2021-10-1-3.
- [21] K. Tamalmani and H. Husin, "Applied sciences review on corrosion inhibitors for oil and gas corrosion issues," *Applied Sciences*, vol. 10, no. 10, p. 3389, 2020, doi: 10.3390/app10103389.
- [22] D. A. Winkler et al., "Impact of inhibition mechanisms, automation, and computational models on the discovery of organic corrosion inhibitors," *Prog Mater Sci*, vol. 149, no. July 2024, 2025, doi: 10.1016/j.pmatsci.2024.101392.
- [23] S. Sivalingam, M. Rajendran, J. Gayathri, S. Anu, J. Kavirajwar, and M. Ghosh, "A novel green synthesis of ZrO nanoparticles as a corrosion inhibitor on ASTM-415 carbon steel in 0.5 M H<sub>2</sub>SO<sub>4</sub>," *Results Chem*, vol. 12, no. August, p. 101877, 2024, doi: 10.1016/j.rechem.2024.101877.
- [24] T. Adistantria Mariami, B. Antoko, and S. Soim, "Analisis laju korosi dan lifetime pipa ASTM A105 dengan perbandingan inhibitor NaNO<sub>2</sub> dan Na<sub>2</sub>CrO<sub>4</sub>," *Proceeding 4rd Conference of Piping Engineering and its Application*, no. 2656, pp. 254–259, 2019.
- [25] M. A. Abbas, K. Zakaria, A. M. El-shamy, S. Zein, and E. Abedin, "Utilization of 1-butylpyrrolidinium chloride ionic liquid as an eco-friendly corrosion inhibitor and biocide for oilfield equipment : combined weight loss , electrochemical and SEM studies," *International Journal of Research In Physical Chemistry and Chemical Physics*, vol. 235, no. 4, pp. 1–30, 2019, doi: 10.1515/zpch-2019-1517.
- [26] R. Rahmaniah, S. R. A. Rani, K. Abidin, and ..., "Pengaruh penambahan inhibitor alami ekstrak limbah kulit jagung terhadap laju korosi material baja ST 37 dalam medium NaCl 3%," *Teknosains: Media Informasi Sains dan Teknologi*, vol. 17, no. 1, pp. 116–127, 2023, doi: 10.24252/teknosains.v17i1.35191.
- [27] L. T. Popoola, "Organic green corrosion inhibitors (OGCIs): A critical review," *Corrosion Reviews*, vol. 37, no. 2, pp. 71–102, 2019, doi: 10.1515/correv-2018-0058.
- [28] D. Singh, M. A. Quraishi, and A. Quraishi, "Recent trends in environmentally sustainable Sweet corrosion inhibitors," *J Mol Liq*, vol. 326, p. 115117, 2021, doi: 10.1016/j.molliq.2020.115117.
- [29] I. M. Khan, R. Rahman, A. Mushtaq, and M. Rezgui, "Hibiscus rosa-sinensis L. (Malvaceae) : Distribution, chemistry and uses," *IJCBS*, no. 12, 2019. [Online]. Available: <https://www.iscientific.org/wp-content/uploads/2019/10/14-IJCBS-17-12-14.pdf>
- [30] S. Nandi, K. Y. Gaidhani, and P. D. Khurpade, "Hibiscus leaves extract: A green corrosion inhibitor," *J. Indian Chem. Soc.*, vol. 97, pp. 865–869, 2020. [Online]. Available: <https://www.researchgate.net/publication/347424336>
- [31] J. J. Mejia, L. J. Sierra, J. G. Ceballos, J. R. Martinez, and E. E. Stashenko, "Color, antioxidant capacity and flavonoid composition in *Hibiscus rosa-sinensis* cultivars," *Molecules*, vol. 28, no. 4, p. 1779, 2023, doi: 10.3390/molecules28041779.
- [32] C. Amabuo, V. U. Wachikwu-Elechi, and S. S. Ikiensikimama, "Corrosion inhibition using *Hibiscus rosa-sinensis* extract for mild steel in an acidic medium," in *SPE Nigeria Annual International Conference and Exhibition*, Nigeria, Aug. 2024, Paper no. SPE-221765-MS, doi: 10.2118/221765-MS.
- [33] B. Latha, K. Kavitha, and S. Rajendran, "Inhibition of corrosion of mild steel in simulated oil well water by aqueous extract of *Hibiscus rosa-sinensis* flower," *Materials Protection*, vol. 65, no. 1, pp. 86–96, 2024, doi: 10.62638/ZasMat1005.
- [34] S. Razvarz, R. Jafari, and A. Gegov, *Flow Modelling and Control in Pipeline Systems: A Formal Systematic Approach*. Cham, Switzerland: Springer Nature, 2021, doi: 10.1007/978-3-030-59246-2.
- [35] ACE/ASTM, *Standard Guide for Laboratory Immersion Corrosion Testing of Metals*, ASTM International, West Conshohocken, PA, USA, 2021.
- [36] ASTM G106-99(1999), *Standard Practice for Verification of Algorithm and Equipment for Electrochemical Impedance Measurements*, ASTM International, West Conshohocken, PA, USA, 1999.
- [37] S. Wan, H. Chen, T. Zhang, B. Liao, and X. Guo, "Anti-corrosion mechanism of parsley extract and synergistic iodide as novel corrosion inhibitors for carbon steel-Q235 in acidic medium by electrochemical, XPS and DFT methods," *Front Bioeng Biotechnol*, vol. 9, Dec. 2021, doi: 10.3389/fbioe.2021.815953.
- [38] S. Sivalingam, M. Rajendran, J. Gayathri, S. Anu, J. Kavirajwar, and M. Ghosh, "A novel green synthesis of ZrO nanoparticles as a corrosion inhibitor on ASTM-415 carbon steel in 0.5 M H<sub>2</sub>SO<sub>4</sub>," *Results Chem*, vol. 12, Dec. 2024, doi: 10.1016/j.rechem.2024.101877.

## ORIGINALITY REPORT

8%

SIMILARITY INDEX

7%

INTERNET SOURCES

6%

PUBLICATIONS

0%

STUDENT PAPERS

## PRIMARY SOURCES

1	<a href="https://www.thejournalshouse.com">thejournalshouse.com</a> Internet Source	2%
2	<a href="https://dokumen.pub">dokumen.pub</a> Internet Source	2%
3	<a href="https://www.mdpi.com">www2.mdpi.com</a> Internet Source	1%
4	S.K. Dhawan, Hema Bhandari, Gazala Ruhi, Brij Mohan Singh Bisht, Pradeep Sambyal. "Corrosion Preventive Materials and Corrosion Testing", CRC Press, 2020 Publication	<1%
5	Karan Sotoodeh. "Industrial Valves", Wiley, 2023 Publication	<1%
6	"Grafted Biopolymers as Corrosion Inhibitors", Wiley, 2023 Publication	<1%
7	<a href="https://www.nature.com">www.nature.com</a> Internet Source	<1%
8	<a href="https://core.ac.uk">core.ac.uk</a> Internet Source	<1%
9	<a href="https://jurnal.untirta.ac.id">jurnal.untirta.ac.id</a> Internet Source	<1%
10	<a href="https://www.mdpi.com">www.mdpi.com</a> Internet Source	<1%
11	Felipe M. Galleguillos Madrid, Alvaro Soliz, Luis Cáceres, Markus Bergendahl et al. "Green Corrosion Inhibitors for Metal and Alloys	<1%

# Protection in Contact with Aqueous Saline", Materials, 2024

Publication

12

ebin.pub  
Internet Source

<1%

Exclude quotes On

Exclude matches < 17 words

Exclude bibliography On